Journal of the Physical Society of Japan
Vol. 76, No. 5, May, 2007, 054802

Generation of Macroscopic Entangled States in Coupled Superconducting Phase Qubits

Shigemasa MATSUO[1], Sahel ASHHAB[2], Toshiyuki FUJII[3], Franco NORI[2,4], Katsuhiko NAGAI[1,3], and Noriyuki HATAKENAKA[1,5]

[1]*Graduate School of Integrated Arts and Sciences, Hiroshima University, Higashi-Hiroshima, Hiroshima 739-8521*
[2]*Frontier Research System, The Institute of Physical and Chemical Research (RIKEN), Wako, Saitama 351-0198*
[3]*AdSM, Hiroshima University, Higashi-Hiroshima, Hiroshima 739-8530*
[4]*Center for Theoretical Physics, Physics Department, CSCS, The University of Michigan, Ann Arbor, MI 48109-1040, U.S.A.*
[5]*MILq Project, International Project Center for Integrated Research on Quantum Information and Life Science, Higashi-Hiroshima, Hiroshima 739-8530*

(Received February 19, 2007; accepted March 16, 2007; published May 10, 2007)

We consider the possibility of generating macroscopic entangled states in capacitively coupled phase qubits. First we discuss the operation of phase qubits and the implementation of the basic gate operations in them. We then analyze two possible procedures that can be used to generate n-qubit entangled states, such as the Greenberger–Horne–Zeilinger state for the case $n = 3$. The procedures we propose are constructed under the experimentally motivated constraint of trying to minimize the number of control lines used to manipulate the qubits.

KEYWORDS: phase qubit, quantum circuit, entangled states, Greenberger–Horne–Zeilinger state
DOI: 10.1143/JPSJ.76.054802

1. Introduction

Entangled states have attracted attention and caused controversy for several decades.[1,2] The first experimental observations of entanglement were performed in optical systems involving photons.[3] A natural extension to those experiments was the search for entanglement in larger and larger objects, and some observations of entanglement in such large systems (e.g., collective spins of gaseous samples[4] and Josephson-junction based quantum circuits[5–11]) have been performed.

One clear motivation to study entanglement in Josephson-junction based circuits is the fact that they are presently studied as candidates for quantum information processing devices[12] (we shall use the word qubits to refer to the basic two-level systems in these circuits). Their main advantages are their inherent scalability using well-established microfabrication techniques and ease of access, for both manipulation and readout, using bias currents, gate voltages and magnetic fields. Strong evidence for two-qubit entanglement[5–7,11] and evidence of four-qubit entangled eigenstates[10] have already been observed, and methods for generating multi-qubit entangled states have been proposed.[13–15]

Given unlimited controls on the qubits in the circuit, one can come up with various methods to prepare multi-qubit entangled states, e.g., the Greenberger–Horne–Zeilinger (GHZ) state of three entangled qubits.[16] In practice, however, every additional control line adds complexity and noise to the system. As a result, the more control lines one uses, the more difficult it is to observe quantum behaviour, such as entanglement, in the circuit. We therefore seek preparation schemes of entangled states using as few and simple control circuit elements as possible, even if we are forced to use somewhat long procedures. That is in fact one of the main reasons why here we study phase qubits.[6,7,17,18] In the proposals that we shall explain below, which are essentially modified versions of atomic-physics and trapped-ion proposals, only dc pulses of bias current to all the qubits and Rabi oscillations in one junction will be required. Furthermore, fast and reliable readout schemes have been developed for this kind of qubits recently (see, e.g., ref. 19). A constraint that must also be kept in mind when devising a preparation scheme is the fact that inter-qubit coupling strengths in superconducting circuits are usually fixed. One must therefore devise methods to perform the required operations without having to tune *in situ* those coupling strengths.[20]

We analyze two different schemes for generating multi-qubit entangled states. The first approach is due to Cirac and Zoller[21] (note that this proposal is entirely different from the Cirac–Zoller proposal for manipulating trapped ions) and seems to be particularly useful for the generation of the GHZ state. The second approach is inspired by a method used by Monroe *et al.*[22] to perform two-qubit operations on trapped ions, and it is better suited for generating entangled states involving a larger number of qubits.

One may ask why it is worth studying the generation of the GHZ state. In contrast to two-qubit entangled states, where the evidence for entanglement is obtained by analyzing the statistics of a large number of measurements and comparing the results with the Bell inequality, the GHZ state gives different predictions from unentangled states even in a single run of the experiment.[16,23] Furthermore, generating the GHZ state can be considered a first step towards generating cluster states and other many-qubit entangled states, which play a crucial role in quantum information processing applications.

This paper is organized as follows: In §2 we present a circuit of capacitively coupled phase qubits and the

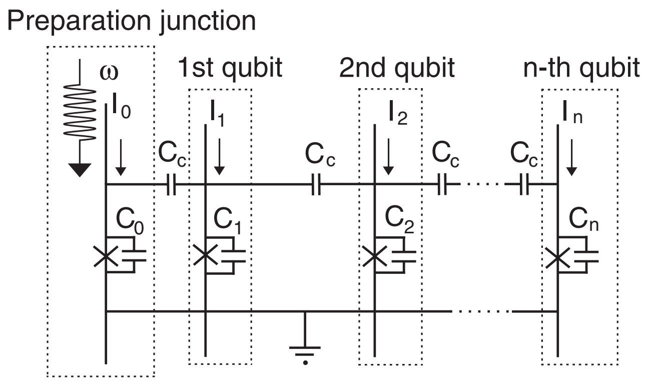

Fig. 1. Circuit consisting of a preparation junction and n capacitively coupled phase qubits.

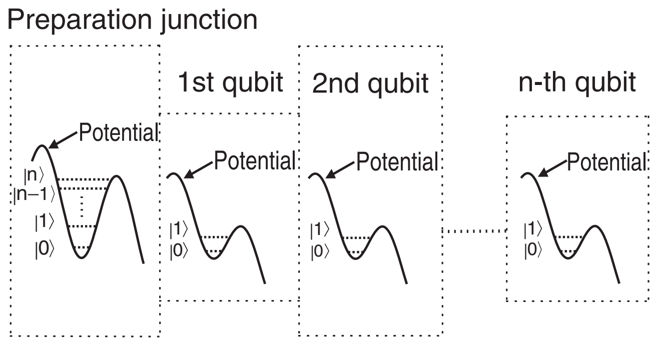

Fig. 2. Schematic diagram of the (tilted-washboard) effective potential for the phase variable of the preparation junction and the n qubits. The dotted lines represent the quantum states that will be used below.

Hamiltonian that describes it. In §3 we introduce the basic gate operations that will be used in the generation of multi-qubit entangled states. The entangled-state preparation procedures are detailed in §4 and 5. Section 6 contains numerical estimates for possible experimental implementations and some concluding remarks.

2. Hamiltonian

Let us consider a set of $n+1$ Josephson junctions that are connected via capacitances C_c, as shown in Fig. 1. This system can, for our purposes, be described using the Hamiltonian

$$H = \sum_{i=0}^{n} H_i + \sum_{i=0}^{n-1} V_{i,i+1}, \tag{1}$$

where

$$H_i = \frac{p_i^2}{2m_i} + E_{Ji}\left[\left(1-\cos\gamma_i\right) - \frac{I_i}{I_{ci}}\gamma_i\right], \tag{2}$$

$$V_{i,i+1} = \frac{p_i p_{i+1}}{m_{i,i+1}}. \tag{3}$$

The first term in the single-junction Hamiltonian (2) is the effective charging energy of the i-th junction, and it is expressed in such a way to show that the charge variable is the canonical momentum of the phase variable γ_i, in particular classically one finds that

$$p_i \simeq C_i\left(\frac{\Phi_0}{2\pi}\right)^2 \dot{\gamma}_i. \tag{4}$$

The effective mass is

$$m_i \simeq C_i\left(\frac{\Phi_0}{2\pi}\right)^2, \tag{5}$$

C_i is the capacitance of the i-th junction, and $\Phi_0 = h/2\mathrm{e}$ is the flux quantum. E_{Ji} is the Josephson coupling energy

$$E_{Ji} = \frac{\Phi_0}{2\pi} I_{ci}, \tag{6}$$

where I_{ci} is the critical current in the i-th junction. I_i is the bias current applied to the i-th junction. As mentioned above, γ_i is the phase difference across the i-th junction, and $\dot{\gamma}_i$ is its time derivative. The voltage difference across the i-th junction is given by $(\Phi_0/2\pi)^2\dot{\gamma}_i$.

As is well known, a current-biased Josephson junction [as described by eq. (2)] can be represented by a model of a particle in a one-dimensional tilted-washboard potential. When the junction capacitance C_i is small, the effective mass (5) is also small, and the junction can be regarded as a quantum particle. As a result, quantized energy levels can be resolved in the potential. The number of energy levels and energy spacing can be controlled by the bias current I_i. Under an appropriate bias I_i, the junction is well represented by a quantum two-level system, and in that case it is often called a phase qubit.

The second term in the Hamiltonian (1), i.e., $V_{i,i+1}$, is the effective coupling Hamiltonian between the i-th junction and the $(i+1)$-th junction. The coupling constant is

$$m_{i,i+1} \simeq \left(\frac{\Phi_0}{2\pi}\right)^2 \frac{C_i C_{i+1}}{C_c}. \tag{7}$$

Note that here we are making the experimentally relevant assumption that $C_i \gg C_c$, such that only nearest-neighbour interaction terms need to be considered.

In the following, we shall take the junctions with $i = 1, 2, \ldots, n$ to be biased such that they function as phase qubits, with two relevant energy levels. The 0th junction is the preparation junction for the generation of entangled states on the qubits. The biasing conditions for the 0th junction will differ in the two methods that we analyze below. The biasing conditions are illustrated in Fig. 2. The Hamiltonian (1) can now be rewritten using the eigenstates $|k\rangle_i$ of the Hamiltonian (2), which are defined by the eigenvalue problem

$$H_i|k\rangle_i = E_{i,k}(I_i)|k\rangle_i, \tag{8}$$

where i denotes the junction ($i = 0, 1, 2, \ldots, n$), and k is the quantum number describing the quantum state of a given junction (note that the eigenvalues $E_{i,k}$ depend on the bias currents I_i; note also that the slow leakage of the quantum state outside the qubit basis can be treated along with decoherence effects). Since the junctions with $i = 1, 2, \ldots, n$ have two levels each, we can express their Hamiltonians using the Pauli matrices $\sigma_\alpha^{(i)}$ with $\alpha = x, y, z$

$$H_i = \epsilon_i(I_i)\sigma_z^{(i)}, \tag{9}$$

where $\epsilon_i = E_{i,1} - E_{i,0}$. Using the eigenvalue equations (8) and the rotating-wave approximation, we obtain the transformed Hamiltonian

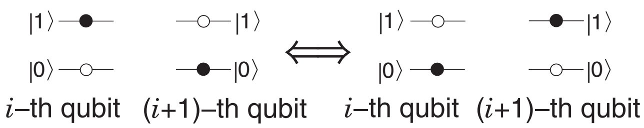

Fig. 3. Schematic diagram of the on-resonance dynamics of the i-th and $(i+1)$-th qubits.

$$\begin{aligned}\hat{H} = &\sum_{k=0}^{n} E_{0,k}(I_0)|k\rangle_0\langle k|_0 + \sum_{i=1}^{n}\epsilon_i(I_0)\sigma_z^{(i)} \\ &+ \sum_{k=1}^{n}\left(\bar{V}_{0,1}^{(k)}|k-1\rangle_0\langle k|_0 \otimes \sigma_+^{(1)} + \text{H.c.}\right) \\ &+ \sum_{i=1}^{n-1}\left(\bar{V}_{i,i+1}\sigma_-^{(i)} \otimes \sigma_+^{(i+1)} + \text{H.c.}\right), \qquad (10)\end{aligned}$$

where

$$\bar{V}_{0,1}^{(k)} = \langle k-1|_0 \otimes \langle 1|_1 V_{0,1}|k\rangle_0 \otimes |0\rangle_1, \qquad (11)$$

$$\bar{V}_{i,i+1} = \langle 0|_i \otimes \langle 1|_{i+1} V_{i,i+1}|1\rangle_i \otimes |0\rangle_{i+1}. \qquad (12)$$

The Hamiltonian in eq. (10) can now be considered the starting point for the procedures that we describe below.

3. Basic Gate Operations

We now introduce the basic gate operations that will be used below in preparing the multi-qubit entangled states.

3.1 SWAP operation between two qubits ($P_{i,i+1}$)

Let us consider the junctions to be biased such that the i-th and $(i+1)$-th qubits are on reseonance with each other, i.e., $\epsilon_i = \epsilon_{i+1} \equiv \epsilon$. Let us also take all other pairs of neighbouring junctions to be out of resonance with each other, i.e., $|\epsilon_j - \epsilon_{j+1}| \gg \bar{V}_{j,j+1}$ for all $j \neq i$. Apart from the i-th and $(i+1)$-th junctions, all other pairs of junctions are effectively decoupled. We can therefore focus on the dynamics of just the two-qubit system. The effective Hamiltonian of this system is given by

$$\begin{aligned}\hat{H}_{\text{SWAP}} = &\frac{\epsilon}{2}\sigma_z^{(i)} + \frac{\epsilon}{2}\sigma_z^{(i+1)} \\ &+ \bar{V}_{i,i+1}\left(\sigma_-^{(i)} \otimes \sigma_+^{(i+1)} + \text{H.c.}\right) \qquad (13)\end{aligned}$$

Inspection of the above effective Hamiltonian shows that the states $|0\rangle_i \otimes |0\rangle_{i+1}$ and $|1\rangle_i \otimes |1\rangle_{i+1}$ do not evolve with time, apart from the evolution of their phase factors. The states $|0\rangle_i \otimes |1\rangle_{i+1}$ and $|1\rangle_i \otimes |0\rangle_{i+1}$, on the other hand, perform flip-flop processes, as shown in Fig. 3. If the system is allowed to evolve under the effect of this effective Hamiltonian for a period of time given by

$$\Delta t_{i,i+1}^{\text{SWAP}} = \frac{\pi}{2}\frac{\hbar}{|\bar{V}_{i,i+1}|}, \qquad (14)$$

an i-SWAP operation is performed between the two qubits.[24] In the special case when one of the qubits is in its ground state, the i-SWAP operation simply swaps the quantum states between the two qubits (up to a simple phase factor).

3.2 Generalized SWAP operation between preparation junction and 1st qubit ($P_{0,1}^{(k)}$)

Let us now consider the junctions to be biased such that $\epsilon_1 = E_{0,k} - E_{0,k-1}$, with all pairs of neighbouring qubits out of resonance with each other. Using similar arguments to those given in §3.1, we find that by waiting for a time given by $\hbar\pi/2|\bar{V}_{0,1}^{(k)}|$ the amplitudes of the states $|k\rangle_0 \otimes |0\rangle_1$ and $|k-1\rangle_0 \otimes |1\rangle_1$ are swapped (up to phase factors).

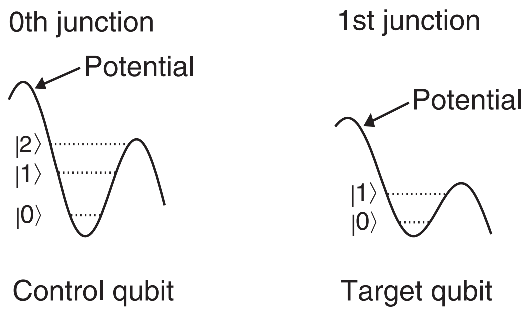

Fig. 4. Schematic diagram of the effective potential for the control and target qubits for the CNOT gate.

3.3 Controlled-NOT operation between preparation junction and 1st qubit ($Q_{0,1}$)

We now present a CNOT gate the flips the 1st qubit, which is called the target qubit in this context, if the preparation junction is in state $|1\rangle_0$. The method we use is inspired by a CNOT gate that was demonstrated with trapped ions[22] (see also ref. 25). In this case, we take the preparation junction to have only three relevant energy levels, as shown in Fig. 4. The procedure now goes as follows:

(1) A $\pi/2$ pulse is applied to the target qubit.

(2) The junctions are biased such that $\epsilon_1 = E_{0,2} - E_{0,1}$ (with no other resonance conditions) and allowed to evolve freely for a period of time given by:

$$\Delta t_{0,1}^{\text{CNOT}} = \pi\frac{\hbar}{|\bar{V}_{0,1}^{(2)}|}. \qquad (15)$$

The effect of this step can be understood by considering the following two cases: (1) If the preparation junction is in the state $|1\rangle_0$ and the target qubit is in the state $|1\rangle_1$, a resonance occurs corresponding to flip-flop processes between the states $|1\rangle_0 \otimes |1\rangle_1$ and $|2\rangle_0 \otimes |0\rangle_1$, and after a full rotation a phase factor of $e^{i\pi}$ is added to the quantum state. (2) If the preparation junction and target qubit are in any of the three other states of the eigenbasis, no resonance occurs, and no extra phase factors are added. This step can therefore be thought of as a controlled-phase gate.[25]

(3) A $\pi/2$ pulse opposite in direction to the one in step 1 is applied to the target qubit. If the preparation junction is in state $|0\rangle_0$, the target qubit goes back to its original state. If the preparation junction is in state $|1\rangle_0$, the additional phase factor from step 2 causes the two $\pi/2$ rotations to add up in the same direction, resulting in an effective π pulse on the target qubit. The CNOT gate has therefore been realized. The above procedure is also shown schematically in Fig. 5.

We now note that in §5 we will only need to perform the CNOT gate with the target qubit initially in the state $|0\rangle$. One can therefore use a simpler procedure that has the same effect as the CNOT gate in that particular case:

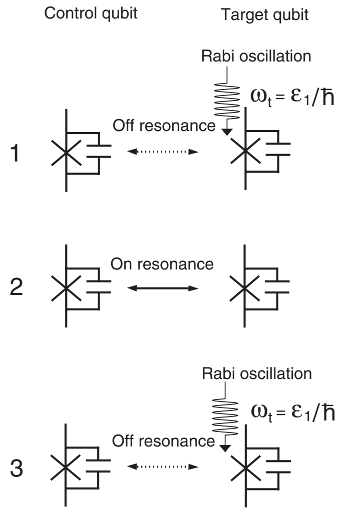

Fig. 5. Procedure for performing the CNOT gate. Each Rabi oscillation step depicted above corresponds to a $\pi/2$ rotation.

(1) A π pulse is applied to the control qubit at frequency $(E_{0,2} - E_{0,1})/\hbar$.
(2) The control and target qubit are brought into resonance with each other and allowed to evolve freely such that the $P_{0,1}^{(2)}$ operation is performed.

The operation of the above procedure can be summarized as follows: $|0\rangle_0|0\rangle_1 \to |0\rangle_0|0\rangle_1 \to |0\rangle_0|0\rangle_1$, and $|1\rangle_0|0\rangle_1 \to |2\rangle_0|0\rangle_1 \to |1\rangle_0|1\rangle_1$.

4. Generation of Multi-Qubit Entangled States I

The first procedure that we propose to use is due to Cirac and Zoller.[21] In order to generate an n-qubit entangled state, the superposition state $(|0\rangle_0 + |n\rangle_0)/\sqrt{2}$ is prepared in the 0th junction, with all the qubits in their ground states. The above superposition would be very difficult to prepare if the 0th junction energy levels were equally spaced. However, current-biased Josephson junctions are well suited for this preparation process; the nonlinearity in the tilted-cosine potential allows a great amount of freedom in preparing a general state in the junction. For reasonable values of n, this preparation step should be relatively straightforward to implement. From the above initial state, excitations are transferred down the chain of qubits one by one until the n-qubit entangled state is generated. We describe the entire procedure in more detail for the case of generating the GHZ state below.

In order to generate the GHZ state, the following procedure is performed:

(1) From the ground state $|0_0 0_1 0_2 0_3\rangle$, the quantum state $(|0\rangle_0 + |3\rangle_0)/\sqrt{2}$ is generated in the 0th junction by driving Rabi oscillations in that junction. All neighbouring junctions are kept off resonance with each other. We now have as the initial state the superposition state

$$|\Phi_0\rangle = \big(|0\rangle_0 + |3\rangle_0\big)|0\rangle_1|0\rangle_2|0\rangle_3/\sqrt{2}. \quad (16)$$

(2) Using a sequence of the basic gates introduced in §3, we reach the state

$$\begin{aligned}|\Phi_1\rangle &= P_{2,3}P_{1,2}P_{0,1}^{(3)}|\Phi_0\rangle,\\ &= P_{2,3}P_{1,2}P_{0,1}^{(3)}\big(|0\rangle_0 + |3\rangle_0\big)|0\rangle_1|0\rangle_2|0\rangle_3/\sqrt{2},\\ &= P_{2,3}P_{1,2}\big(|0\rangle_0|0\rangle_1 + |2\rangle_0|1\rangle_1\big)|0\rangle_2|0\rangle_3/\sqrt{2},\\ &= P_{2,3}\big(|0\rangle_0|0\rangle_1|0\rangle_2 + |2\rangle_0|0\rangle_1|1\rangle_2\big)|0\rangle_3/\sqrt{2},\\ &= (|0\rangle_0|0\rangle_1|0\rangle_2|0\rangle_3 + |2\rangle_0|0\rangle_1|0\rangle_2|1\rangle_3)/\sqrt{2}. \quad (17)\end{aligned}$$

(3) Similarly we perform a sequence of basic gates to reach the state

$$\begin{aligned}|\Phi_2\rangle &= P_{1,2}P_{0,1}^{(2)}|\Phi_1\rangle,\\ &= P_{1,2}P_{0,1}^{(2)}(|0\rangle_0|0\rangle_1|0\rangle_2|0\rangle_3 + |2\rangle_0|0\rangle_1|0\rangle_2|1\rangle_3)/\sqrt{2},\\ &= P_{1,2}\big(|0\rangle_0|0\rangle_1|0\rangle_2|0\rangle_3 + |1\rangle_0|1\rangle_1|0\rangle_2|1\rangle_3\big)/\sqrt{2},\\ &= (|0\rangle_0|0\rangle_1|0\rangle_2|0\rangle_3 + |1\rangle_0|0\rangle_1|1\rangle_2|1\rangle_3)/\sqrt{2}. \quad (18)\end{aligned}$$

(4) We now have a GHZ state involving the 0th, 2nd and 3rd qubits. If one wishes to transfer the quantum state from the 0th to the 1st qubit, e.g. for readout purposes, one can perform the following step

$$\begin{aligned}|\Phi_3\rangle &= P_{0,1}^{(1)}|\Phi_2\rangle,\\ &= P_{0,1}^{(1)}\big(|0\rangle_0|0\rangle_1|0\rangle_2|0\rangle_3 + |1\rangle_0|0\rangle_1|1\rangle_2|1\rangle_3\big)/\sqrt{2},\\ &= (|0\rangle_0|0\rangle_1|0\rangle_2|0\rangle_3 + |0\rangle_0|1\rangle_1|1\rangle_2|1\rangle_3)/\sqrt{2},\\ &= |0\rangle_0\big(|0\rangle_1|0\rangle_2|0\rangle_3 + |1\rangle_1|1\rangle_2|1\rangle_3\big)/\sqrt{2}. \quad (19)\end{aligned}$$

As a result, the GHZ state is generated in the 1st, 2nd and 3rd qubits. The generalization of the above procedure to n qubits is straightforward.

5. Generation of Multi-Qubit Entangled States II

Although the procedure given in §4 is simple and requires a small number of gates, it would be difficult to apply it in the case many qubits. The difficulty arises because of the restriction on the number of energy levels in the preparation junction; the more energy levels there are in the junction, the less nonlinear it is. As a result, the preparation of the initial superposition state would be hampered. In this section, we propose an alternative scheme for generating such many-qubit entangled states using the CNOT and SWAP gate operations. This scheme is inspired by one that is due to Monroe *et al.*[22]

The basic idea is the following: the superposition state $(|0\rangle_0 + |1\rangle_0)/\sqrt{2}$ is generated in the preparation junction, while all the qubits are in their ground states $|0\rangle_i$. After performing a CNOT gate on the 1st qubit, the state of this two-junction system is the entangled state $(|0\rangle_0|0\rangle_1 + |1\rangle_0|1\rangle_1)/\sqrt{2}$. The state of the 1st qubit is then transferred to the n-th qubit by using SWAP gates. The process is repeated n times, and a many-qubit entangled state is generated (note that the preparation junction, which can also be called the control qubit in this context, is part of the entangled state). In order to illustrate how the generation scheme works, we explain it for the case of the GHZ state below.

The procedure for generating the GHZ state is depicted in Fig. 6. Three junctions are used, including the preparation junction (or control qubit), and the following procedure is carried out:

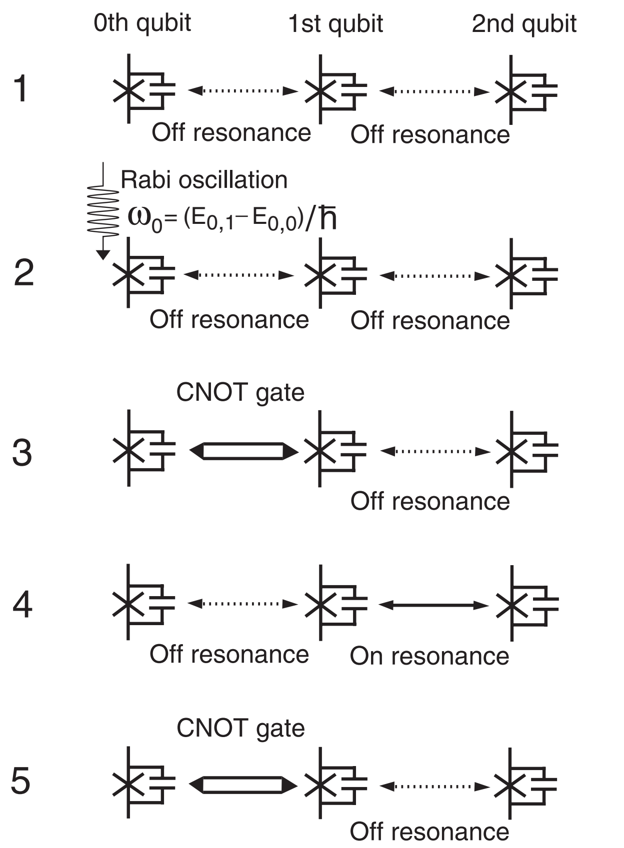

Fig. 6. Procedure for generating the GHZ state by using CNOT gate operations. The Rabi oscillation step depicted above corresponds to a $\pi/2$ rotation.

(1) We start with the ground state

$$|\Phi_0\rangle = |0\rangle_0|0\rangle_1|0\rangle_2, \tag{20}$$

and all three junctions are kept off resonance with each other.

(2) Using Rabi oscillations, a superposition state is generated in the 0th qubit:

$$|\Phi_1\rangle = (|0\rangle_0 + |1\rangle_0)|0\rangle_1|0\rangle_2/\sqrt{2}. \tag{21}$$

(3) A CNOT gate is performed on the 1st qubit using the 0th qubit as the control qubit, such that the quantum state evolves into

$$\begin{aligned}|\Phi_2\rangle &= Q_{0,1}|\Phi_1\rangle\\ &= (|0\rangle_0|0\rangle_1 + |1\rangle_0|1\rangle_1)|0\rangle_2/\sqrt{2}.\end{aligned} \tag{22}$$

(4) The state of the 1st qubit is transferred to the 2nd qubit using the SWAP gate, such that the quantum state evolves into

$$\begin{aligned}|\Phi_3\rangle &= P_{1,2}|\Phi_2\rangle,\\ &= P_{1,2}(|0\rangle_0|0\rangle_1|0\rangle_2 + |1\rangle_0|1\rangle_1|0\rangle_2)/\sqrt{2},\\ &= (|0\rangle_0|0\rangle_1|0\rangle_2 + |1\rangle_0|0\rangle_1|1\rangle_2)/\sqrt{2}.\end{aligned} \tag{23}$$

(5) A CNOT gate is performed on the 1st qubit using the 0th qubit as the control qubit:

$$\begin{aligned}|\Phi_4\rangle &= Q_{0,1}|\Phi_3\rangle,\\ &= Q_{0,1}(|0\rangle_0|0\rangle_1|0\rangle_2 + |1\rangle_0|0\rangle_1|1\rangle_2)/\sqrt{2},\\ &= (|0\rangle_0|0\rangle_1|0\rangle_2 + |1\rangle_0|1\rangle_1|1\rangle_2)/\sqrt{2}.\end{aligned} \tag{24}$$

As a result, the GHZ state is generated. The generalization of the above procedure to the case of n qubits is straightforward.

6. Discussion

We first estimate in general terms the time required to perform the above procedures. The slowest step in this setup is typically determined by inter-qubit coupling, which is chosen to be weak in order to achieve effective decoupling between the qubits out of resonance. In the first preparation procedure, $n(n-1)/2$ SWAP operations are required to generate the n-qubit entangled state [the number of operations is $n(n+1)/2$ if we use the modified version of it; see §4]. Therefore, a three-qubit entangled state would require six SWAP operations. In the second procedure, $n-1$ CNOT gates and $(n-1)(n-2)/2$ SWAP operations are required, giving a total of $n(n-1)/2$ coupling-based operations (note that a CNOT gate and a SWAP operation take roughly the same amount of time). For example, four-, five- and six-qubit entangled states would require six, ten and fifteen operations, respectively. One should also note that Rabi oscillation frequencies typically should not exceed a few percent of the qubit characteristic frequencies, in order to avoid leakage and driving undesired transitions. However, even when that Rabi-oscillation steps are as slow as coupling-based steps, we find that four-, five- and six-qubit entangled states would require ten, fifteen and twenty one operations, respectively. Fast dc pulses can be applied with negligible errors.[26)]

In an experimental setup with phase qubits, the qubit characteristic frequencies are typically of the order of 10 GHz. The decoherence times are approaching the microsecond range.[27)] Therefore, in order to perform a sequence of about 10–20 basic operations (which would be required for 4–6 qubits), one would need to have the coupling strengths $\bar{V}_{i,i+1}$ to be larger than ~50 MHz, which is the case for current experimental situations.[7,19)] The ratio between the self capacitance C_i and the coupling capacitance C_c is[19)] roughly 100, justifying the nearest-neighbour approximation to the interaction energy. The bias currents can be modulated at rates (of the order of 1 ns) that are adiabatic with respect to the internal states of the separate qubits, but instantaneous with respect to the coupling energies. Although the above estimates are not taken from the same experiment, they show that the parameters required for the experimental implementation of our proposals are all realistic.

In conclusion, we have proposed two different schemes to generate multi-qubit entangled states in capacitively coupled phase qubits, keeping in mind the experimentally motivated constraint of minimizing the number of control lines used to manipulate the qubits. The first proposal is well suited for the generation of the three-qubit GHZ state, whereas the second proposal is well suited for larger systems. Combined with recently developed reliable readout schemes (see, e.g., ref. 19), our simple proposals could be used to achieve the generation of multi-qubit entangled states in phase qubits.

Acknowledgments

We would like to thank L. F. Wei for useful discussions. This work was supported in part by a Grand-in-Aid for Scientific Research (18540352) and for Scientific Research on Priority Areas (17071009) from the Ministry of Education Culture, Sports, Science and Technology of Japan, the National Security Agency (NSA), the Laboratory for Physical Sciences (LPS) and the Army Research Office (ARO); and also by the National Science Foundation (NSF) grant No. EIA-0130383. One of us (S.A.) was supported by the Japan Society for the Promotion of Science (JSPS).

1) E. Schrödinger: Naturwissenschaften **23** (1935) 809; E. Schrödinger: Proc. Cambridge Philos. Soc. **31** (1935) 555; E. Schrödinger: Proc. Cambridge Philos. Soc. **32** (1936) 446.
2) A. Einstein, B. Podolsky, and N. Rosen: Phys. Rev. **47** (1935) 777; N. Bohr: Phys. Rev. **48** (1935) 696.
3) See, e.g., A. Aspect, P. Grangier, and G. Roger: Phys. Rev. Lett. **47** (1981) 460; and references therein for previous experiments.
4) B. Julsgaard, A. Kozhekin, and E. S. Polzik: Nature **413** (2001) 400.
5) Yu. A. Pashkin, T. Yamamoto, O. Astafiev, Y. Nakamura, D. V. Averin, and J. S. Tsai: Nature **421** (2003) 823; Yu. A. Pashkin, T. Yamamoto, O. Astafiev, Y. Nakamura, D. V. Averin, T. Tilma, F. Nori, and J. S. Tsai: Physica C **426** (2005) 1552.
6) P. R. Johnson, F. W. Strauch, A. J. Dragt, R. C. Ramos, C. J. Lobb, J. R. Anderson, and F. C. Wellstood: Phys. Rev. B **67** (2003) 020509.
7) A. J. Berkley, H. Xu, R. C. Ramos, M. A. Gubrud, F. W. Strauch, P. R. Johnson, J. R. Anderson, A. J. Dragt, C. J. Lobb, and F. C. Wellstood: Science **300** (2003) 1548.
8) A. Izmalkov, M. Grajcar, E. Il'ichev, Th. Wagner, H.-G. Meyer, A. Yu. Smirnov, M. H. S. Amin, A. M. van den Brink, and A. M. Zagoskin: Phys. Rev. Lett. **93** (2004) 037003.
9) H. Xu, F. W. Strauch, S. K. Dutta, P. R. Johnson, R. C. Ramos, A. J. Berkley, H. Paik, J. R. Anderson, A. J. Dragt, C. J. Lobb, and F. C. Wellstood: Phys. Rev. Lett. **94** (2005) 027003.
10) M. Grajcar, A. Izmalkov, S. H. W. van der Ploeg, S. Linzen, T. Plecenik, Th. Wagner, U. Hübner, E. Il'ichev, H.-G. Meyer, A. Yu. Smirnov, P. J. Love, A. M. van den Brink, M. H. S. Amin, S. Uchaikin, and A. M. Zagoskin: Phys. Rev. Lett. **96** (2006) 047006.
11) M. Steffen, M. Ansmann, R. C. Bialczak, N. Katz, E. Lucero, R. McDermott, M. Neeley, E. M. Weig, A. N. Cleland, and J. M. Martinis: Science **313** (2006) 1423.
12) For reviews on this subject, see, e.g., Y. Makhlin, G. Schön, and A. Shnirman: Rev. Mod. Phys. **73** (2001) 357; J. Q. You and F. Nori: Phys. Today **58** (2005) No. 11, 42; G. Wendin and V. Shumeiko: in *Handbook of Theoretical and Computational Nanotechnology*, ed. M. Rieth and W. Schommers (ASP, Los Angeles, 2006).
13) C.-P. Yang and S. Han: Phys. Rev. A **70** (2004) 062323.
14) L. F. Wei, Y.-x. Lui, and F. Nori: Phys. Rev. Lett. **96** (2006) 246803.
15) R. Migliore, K. Yuasa, H. Nakazato, and A. Messina: Phys. Rev. B **74** (2006) 104503.
16) D. M. Greenberger, M. Horne, and A. Zeilinger: in *Bell's Theorem, Quantum Theory, and Conceptions of the Universe*, ed. M. Kafatos (Kluwer Academic, Dordrecht, 1989) p. 73; D. M. Greenberger, M. Horne, A. Shimony, and A. Zeilinger: Am. J. Phys. **58** (1990) 1131.
17) Y. Yu, S. Han, X. Chu, S. Chu, and Z. Wang: Science **296** (2002) 889.
18) J. M. Martinis, S. Nam, J. Aumentado, and C. Urbina: Phys. Rev. Lett. **89** (2002) 117901.
19) R. McDermott, R. W. Simmonds, M. Steffen, K. B. Cooper, K. Cicak, K. D. Osborn, S. Oh, O. P. Pappas, and J. M. Martinis: Science **307** (2005) 1299.
20) L. F. Wei, Y.-x. Liu, and F. Nori: Phys. Rev. B **72** (2005) 104516.
21) J. I. Cirac and P. Zoller: Phys. Rev. A **50** (1994) R2799.
22) C. Monroe, D. M. Meekhof, B. E. King, W. M. Itano, and D. J. Wineland: Phys. Rev. Lett. **75** (1995) 4714.
23) See, e.g., N. D. Mermin: Phys. Today **43** (1990) No. 6, 9.
24) A. Blais, A. M. van den Brink, and A. M. Zagoskin: Phys. Rev. Lett. **90** (2003) 127901.
25) F. W. Strauch, P. R. Johnson, A. J. Dragt, C. J. Lobb, J. R. Anderson, and F. C. Wellstood: Phys. Rev. Lett. **91** (2003) 167005.
26) Q. Zhang, A. G. Kofman, J. M. Martinis, and A. N. Korotkov: cond-mat/0607385.
27) J. M. Martinis, K. B. Cooper, R. McDermott, M. Steffen, M. Ansmann, K. D. Osborn, K. Cicak, S. Oh, D. P. Pappas, R. W. Simmonds, and C. C. Yu: Phys. Rev. Lett. **95** (2005) 210503.